BARIUM CONCENTRATIONS AS A PROXY FOR EQUATORIAL PACIFIC PRODUCTIVITY DURING THE PAST 140, 000 YEARS

An Undergraduate Research Scholars Thesis

by

OLUWASEYIFUNMITAN OLANIYI-SHOLANKE

Submitted to the Undergraduate Research Scholars program at
Texas A&M University
in partial fulfillment of the requirements for the designation as an

UNDERGRADUATE RESEARCH SCHOLAR

Approved by Research Advisor: Dr. Franco Marcantonio

May 2017

Major: Geology

TABLE OF CONTENTS

ABSTRACT

Barium Concentrations as a Proxy for Equatorial Pacific Productivity
During the Past 140,000 Years

Oluwaseyifunmitan Olaniyi-Sholanke
Department of Geology & Geophysics
Texas A&M University

Research Advisor: Dr. Franco Marcantonio
Department of Geology & Geophysics
Texas A&M University

The accumulation of biogenic sediments in the deep ocean may yield important information about past ocean productivity and its relationship to climate change. Sediments, sampled at approximately millennial resolution, every 4 – 5 cm on average, were obtained from a core (ML1208-17PC) retrieved from the Central Equatorial Pacific (CEP) ocean (0.48°N,156.45°W; water depth 2,926 m). The main objectives of this research were to (1) use barium concentrations in marine sediments as a proxy for past ocean export production, and to (2) determine how past glacial-interglacial changes in productivity are related to climate and, specifically, variability of dust fluxes which, in turn, are a function of changing atmospheric circulation patterns.

Ba concentrations on complete digestions of bulk sediment were measured by inductively-coupled plasma mass spectrometry. Sediments ranging in age from late Holocene to 140 kyr yielded bulk barium concentrations that ranged from about 305 to 670 ppm. The authigenically-derived portion of the total barium, thought to be correlated with export production, is denoted as the biogenically-derived barium (bioBa). Using accumulation rates

derived by Jacobel et al. (2017), we found bioBa accumulation rates that ranged from about 0.5 to 1.0 mg cm^{-2} kyr^{-1}. For this research, the following hypotheses were tested:

1.) BioBa fluxes (i.e., productivity) will be higher at the equatorial site, during the last glacial maximum (Marine oxygen Isotope stage 2 (MIS 2); i.e. 25 – 12 kyr), than the same fluxes during the MIS 1 (i.e., 12 – 0 kyr).

2.) BioBa fluxes (i.e. productivity) will be higher during glacial MIS 4 and MIS 6 than those during interglacial MIS 3 and MIS 5.

Over the past 140 kyr, there is a positive relationship between productivity and warm interglacial periods which, in turn, are anti-correlated with dust fluxes determined by Jacobel et al. (2017). Thus, high bioBa accumulation rates correspond to less dusty warm periods, and vice versa. Productivity is apparently not a function of dust fertilization in the central equatorial Pacific, on Milankovitch glacial-interglacial timescales.

ACKNOWLEDGEMENTS

I would like to thank my faculty advisor, Dr. Franco Marcantonio, for his guidance and continuous support through the scheme of this research project.

Also, I would like to express my sincere gratitude to Maria Reimi, Mathew Loveley, Luz Romero and Marilyn Wisler for their help and insight through the course of my research.

Finally, thanks to my family for their encouragement and love.

NOMENCLATURE

Ba	Barium
$BaSO_4$	Barite: Barium Sulfate
bioBa	Biogenic barium
CEP	Central Equatorial Pacific
C_{org}	Organic carbon
CO_2	Carbon dioxide gas
$HClO_4$	Perchloric acid
HF	Hydrofluoric acid
HNO_3	Nitric acid
Kyr	Thousand years ago
MIS	Marine oxygen Isotope Stage
MAR	Mass Accumulation Rate
MQ-H_2O	MilliQ water (Distilled water)
NIST	National Institute of Standards and Technology
ppm	parts per million
R/V	Research Vessel
Th	Thorium (232)

CHAPTER I

INTRODUCTION

Background

Barium (Ba) concentrations in marine sediment can be used as a proxy for past ocean productivity and, therefore, in the reconstruction of past climates. In upwelling zones, sediments are characterized with high barite concentrations (Goldberg and Arrhenius, 1958). Barium present in ocean waters is generated through precipitation within areas of decaying biogenic material. The mineral barite ($BaSO_4$) is the main carrier of biogenically-precipitated Ba (hereafter referred to as bioBa) in sediments (Goldberg and Arrhenius, 1958; Dehairs et al., 1980; Dymond et al., 1992). Marine barite consists of approximately 50 -100% of the total non-detrital, solid-phase Ba in the water column (Goldberg and Arrhenius, 1958).

Ba concentrations are higher in nutrient rich waters, implying that the formation of barite is controlled by biota (Dehairs, 1980). In addition, the association of Ba with biogenic material is inferred from Ba-rich sediments that underlie very productive surface waters (Dehairs, 1980). The amount of barite precipitation is highly related to the dissolution of Ba in seawater and the decomposition of organic matter (C_{org}). Because of its association with organic carbon, barite present in marine sediments is commonly used to understand past paleoproductivity levels (Paytan and Griffith, 2007). In addition, barite and bioBa sediment concentrations have been used by geologists to study temporal paleoproductivity changes in the ocean (Dymond et al., 1992), and the relationship these changes have with global climate variability.

The potential of bioBa as a proxy for productivity is significant because barite is well-preserved in marine sediments. The ratio of C_{org} to bioBa decreases with depth in the water

column; this is because with increased bioBa flux, there is a decrease in C_{org} flux. This relationship highlights the viability of barium as a paleoproductivity, and it shows the capability of bioBa to withstand geological processes such as diagenesis (unlike C_{org}), which may recycle material back to the water column (Rushdi et al.,2000).

Productivity Changes and Dust Flux

The growth of phytoplankton in the oceans is intimately associated with the carbon cycle and, therefore, the CO_2 content of the atmosphere and climate variability. When phytoplankton growth rates are high, there is more carbon exported to the deep sea so that CO_2 levels in the atmosphere remain low.

The variability of dust flux is a function of changing atmospheric circulation patterns. High dust fluxes have been associated with glacial time intervals (McGee et al. 2010). Indeed, the cause of the increased dust fluxes may be related to increases in gustiness of the dust sources area, which may characterize glacial periods even at a millennial resolution (McGee et al., 2010). Changes in dust fluxes may play an important role in changing productivity of the oceans through time. When dust dissolves in seawater, it releases iron which is an important micronutrient for phytoplankton growth. One might expect, therefore, that when dust fluxes are high, there may be increased efficiency of the export of CO_2 to the ocean bottom (because of increased productivity), where it is isolated from the surface ocean/atmospheric system.

Costa et al. (2016) assert that the greater dust flux of the last glacial period was not large enough to generate significant iron fertilization and increased productivity. A similar conclusion was reached by Winckler et al. (2016) who additionally suggested that iron, rather than being provided by increased dust fluxes, may be provided to the surface ocean as a result of diffusive and advective upwelling along the equator. Thus, dust fertilization of the ocean may not

contribute to the changing patterns of productivity in the Central Equatorial Pacific (CEP). These hypotheses will be further tested here.

Objectives

The main objectives of this research were to (1) use concentrations of barium in marine sediments as a proxy for past ocean export production, and to (2) determine how past glacial-interglacial changes in productivity are related to climate and, specifically, variability of dust fluxes.

For this research, the following hypotheses were tested:

1.) BioBa fluxes (i.e., productivity) will be higher at the equatorial site, during the last glacial maximum (marine oxygen isotope stage 2 (MIS 2); i.e. 25 – 12 kyr), than the same fluxes during the MIS 1 (i.e., 12 – 0 kyr).

2.) BioBa fluxes (i.e. productivity) will be higher during glacial MIS 4 and MIS 6 than those during interglacial MIS 3 and MIS 5.

CHAPTER II

LOCATION

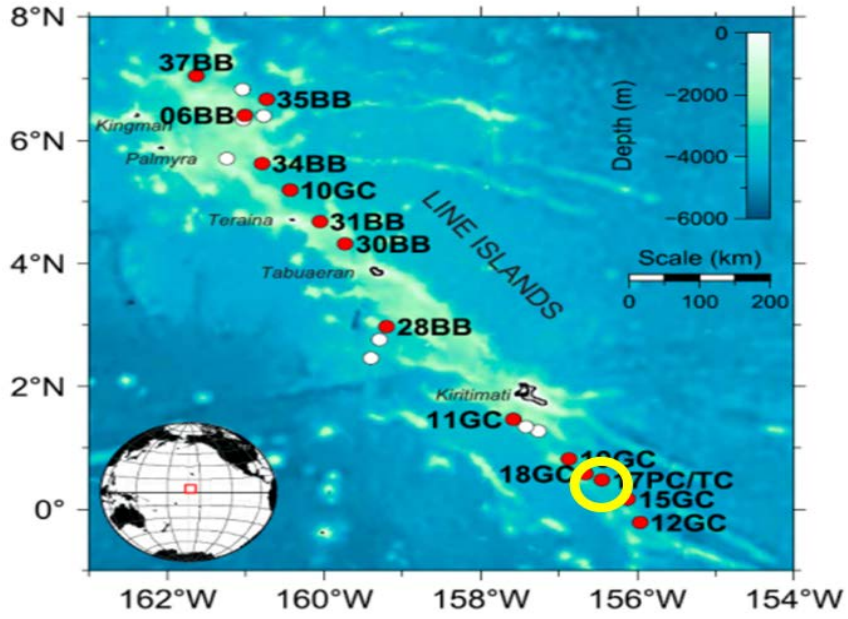

Figure 1: Location of the core: 17PC (yellow circle). Modified from Lynch-Stieglitz et al. (2015).

Sediments, sampled at approximately millennial resolution, were obtained from a core (ML1208-17PC; see location in Figure 1) retrieved from the Central Equatorial Pacific (CEP) (0.48°N,156.45°W; water depth 2,926 m). The study area is in the Line Islands, which form part of series of atolls, seamounts and volcanic ridges. The core studied here (17PC), in addition to several other cores (outlined in Figure 1), were collected by Dr. Jean Lynch-Stieglitz at the Georgia Institute of Technology as part of a research cruise aboard the R/V Marcus Langseth.

CHAPTER III

METHODS

Homogenized sediment samples (~50 mg) were completely digested using a cocktail of HNO_3, HF, and $HClO_4$. Additionally, blanks and NIST standard 2702, run under the same conditions as the sediment samples, were measured as part of this study. Biogenic barium (bioBa) concentrations, defined as the fraction of total Ba not associated with terrigenous material, were estimated by subtracting the concentration of detrital barium from the total measured barium. The detrital fraction of Ba was estimated assuming that the Ba/Th ratio of the sediments is same as the Ba/Th ratio of average upper crust (51.4, i.e., 550 ppm for Ba and 10.7 ppm for Th, Taylor and McLennan, 1985). Therefore, bioBa concentration can be derived by using equation (1):

$$[\text{bioBa}] = [\text{Ba}_{\text{total measured}}]\,[\text{Ba/Th}]_{\text{terrigenous}} * [^{232}\text{Th}] \qquad \text{Eq. (1)}$$

where the ^{232}Th concentration is given for the samples at the same depths in Jacobel et al. (2017). In addition, in order to understand the changes associated with the biogenic barium profile, the bioBa flux was calculated using Eq. (2):

$$\text{bioBa flux} = (\text{bioBa}) * {}^{230}\text{Th-derived sediment Mass Accumulation Rate} \qquad \text{Eq. (2)}$$

where the ^{230}Th-derived sediment Mass Accumulation Rate is given for the same sample intervals in Jacobel et al. (2017).

Apparatus

Equipment used for the pre-digestion, digestion and post-digestion procedures include, an analytical balance, spatula, 50 mL centrifuge tubes, fume hood, 15 mL Savillex beakers and pipette (1000 micro liters).

Acids used were perchloric acid ($HClO_4$), nitric acid (HNO_3) and hydrofluoric acid (HF).

HF and $HClO_4$ broke down the silicates in the samples and HNO_3, an oxidizing agent, promoted further dissolution.

Pre-digestion Procedure

50 mg of the core samples were measured and added to a 15 mL Savillex beaker. The walls of the beakers were rinsed with approximately 0.5 mL MQ-H_2O to dissolve sample. The hot plate was heated to 170^0C and the Savillex beakers containing the samples were placed on the hot plate.

Digestion Procedure

3 mL of $HClO_4$ and 1 mL of HNO_3 were added to the samples consecutively and was left to sit on the hot plate for approximately 40 minutes. Then, 2 mL of HF was added to the samples and left to sit for approximately 20 minutes. The aforementioned step was repeated twice. Lastly, 1 mL of HNO_3 was added to the samples.

Post-Digestion Procedure

The digested samples in the Savillex beakers were transferred to pre-weighed 50 mL centrifuge tubes and filled with MQ-H_2O to the 25 mL mark on the centrifuge tubes.

Concentrations of Ba in the digested samples were measured by inductively-coupled plasma mass spectrometry. Blank corrections were negligible and NIST standard 2702 was accurate to within about 5%.

CHAPTER IV

RESULTS

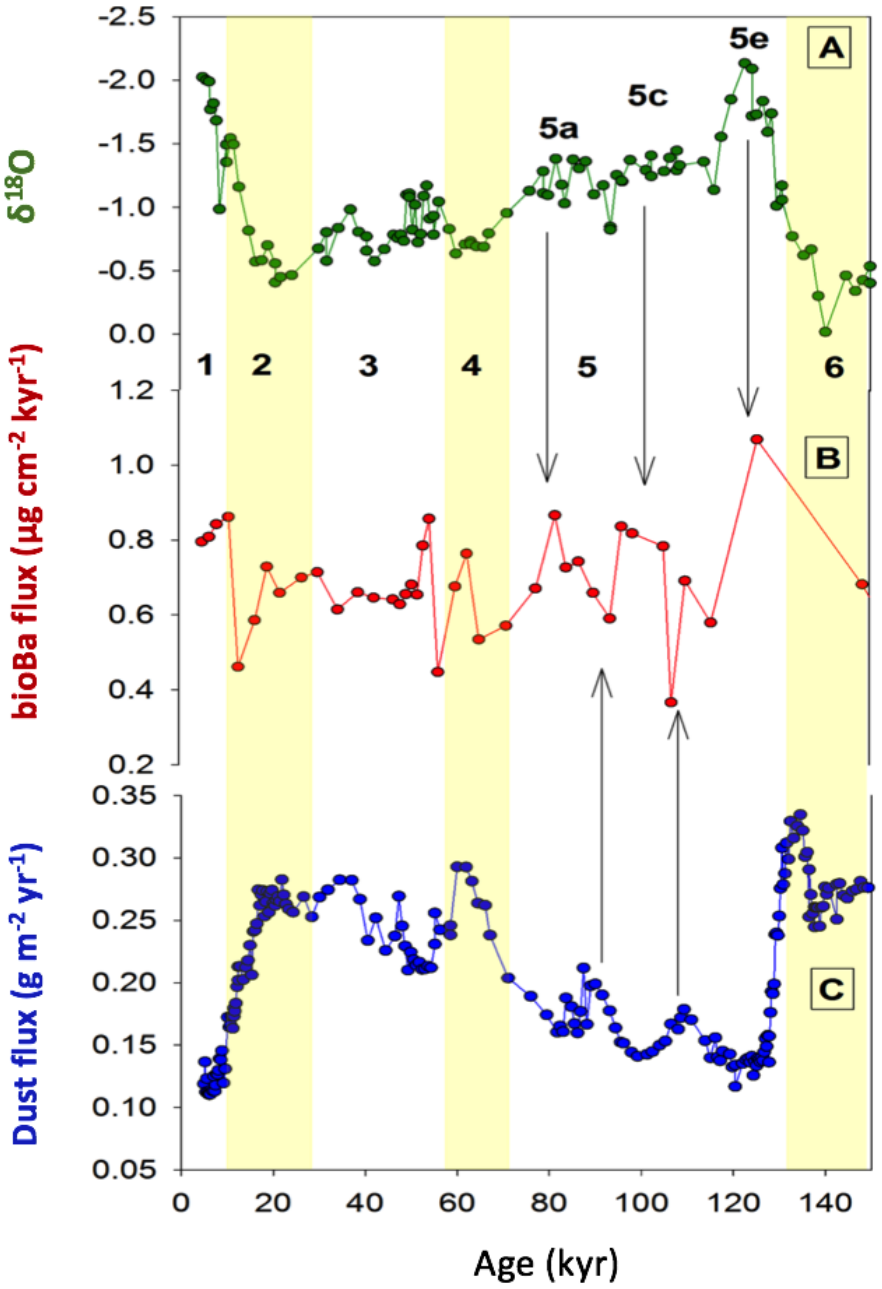

Figure 2. Oxygen isotope curve (A) for core 17PC from Lynch-Stieglitz et al. (2015) and 230Th-derived dust flux (C) from Jacobel et al. (2017). Our BioBa flux (B) in middle panel. Bold numbers represent marine oxygen isotope stages (MIS 1, 3, 5 represent warm interglacial periods and MIS 2, 4, 6 represent cool glacial periods).

The oxygen isotope curve in Figure 2 (oxygen isotope data from Lynch-Stieglitz et al., 2015) was used to determine the chronology of sediments retrieved from core ML1208-17PC. By identifying MIS boundaries, we can understand the temporal paleoproductivity changes in the ocean on a glacial-interglacial timescale.

Sediments ranging in age from late Holocene to 140 kyr yielded bulk barium concentrations that ranged from about 305 to 670 ppm. The authigenically-derived portion of the total barium, thought to be correlated with export production, is denoted as bioBa. The bioBa was estimated by subtracting the lithogenic Ba from the total Ba. Lithogenic Ba contents were calculated using thorium concentrations in the same samples (Jacobel et al., 2017). Our results show that the sediment samples yielded bioBa concentrations ranging from approximately 298 to 662 ppm, and bioBa flux values from approximately 0.447 to 1.068 $\mu g\ cm^{-2}kyr^{-1}$. The bioBa makes up greater than 97% of the total Ba. Using accumulation rates derived by Jacobel et al. (2017), we found bioBa accumulation rates that range from about 0.5 to 1.0 $mg\ cm^{-2}\ kyr^{-1}$.

CHAPTER V

DISCUSSION AND CONCLUSION

In the water column, the covariation of barium abundance and its associated fluxes demonstrate the influence and effects of marine biological cycles. In combination with the flux of organic carbon, bioBa fluxes present in sediment records can be used to infer and characterize paleoproductivity. As shown in Figure 2, there is a positive relationship between productivity (bioBa flux) and warm interglacial periods. In general, productivity is lower during colder periods (MIS 2, 4, and 6) than during warmer periods (MIS 1, 3, 5). Even within interglacial MIS 5, there is a strong precessional relationship with bioBa fluxes (i.e., bioBa flux peaks and troughs correlate with 5a-e).

Dust deposition in the central Equatorial Pacific during the last glacial period (MIS 2) was approximately 2-3 times greater than it was during the Holocene (Jacobel et al., 2017). High glacial dust flux has been recognized to correlate with changes in wind strength, or changes in source aridity (McGee et al. 2010). We find no evidence for high bioBa accumulation rates during the last three glacial time periods (MIS 2, 4, and 6). Instead, we fine the highest bioBa accumulation rates during the warm interglacial periods (MIS 1, 3, and 5), times during which, there was significantly less dust being delivered to the Central Equatorial Pacific Ocean. This is the same pattern identified by Costa et al. (2016) in MIS 1 and MIS 2, although we extend the timing of this finding from 25 kyr to 140 kyr. Costa et al. (2016) believed that the changes in bioBa flux were not related to changes in dust flux because the increase in, dust flux during the last glacial period was not large enough to generate significant iron fertilization to the central Equatorial Pacific. Furthermore, the lack of a positive relationship between our bioBa flux and

dust flux (Figure 2), suggests that nutrients like iron may be provided to the euphotic zone as a result of diffusive and advective upwelling of waters from the Equatorial Undercurrent, as asserted by Winckler et al. (2016). Thus, dust fertilization of the ocean is apparently not contributing to the measure of productivity in the Central Equatorial Pacific (CEP), at least on Milankovitch glacial-interglacial timescales.

REFERENCES

Costa, K. M., McManus, J.F., Anderson, R.F., Winckler, G., Fleisher, M.Q., Ren, H.; Sigman, D.M., Marcantonio, F., Ravelo, A.C., 2016. No iron fertilization in the equatorial Pacific Ocean during the last ice age. *Nature*, 529(7587): 519-522.

Dehairs, F., Chesselet, R., Jedwab, J., 1980. Discrete Suspended Particles of Barite and the Barium Cycle in the Open Ocean. *Earth and Planetary Science Letters*, 49(2): 528-550.

Dymond, J., Suess, E., Lyle, M., 1992. Barium in Deep-Sea Sediment: A Geochemical Proxy for Paleoproductivity. *Paleoceanography*, 7(2): 163-181.

Goldberg, E. D., Arrhenius G.O.S., 1958. Chemistry of Pacific pelagic sediments. *Geochimica et cosmochimica acta*, 13(2).

Jacobel, A., McManus, J., Anderson, R., & Winckler, G., 2017. Climate-related response of dust flux to the central equatorial Pacific over the past 150 kyr, *Earth and Planetary Science Letters*, 45(7): 160-172.

Lynch-Stieglitz, J., P. J. Polissar, A. W. Jacobel, S. A. Hovan, R. A. Pockalny, M. Lyle, R. W. Murray, A. C. Ravelo, S. C. Bova, A. G. Dunlea, et al., 2015. Glacial-interglacial changes in central tropical Pacific surface seawater property gradients. *Paleoceanography*, 30(5): 423-438.

McGee, D., Broecker, W. S., & Winckler, G., 2010. Gustiness: The driver of glacial dustiness? *Quaternary Science Reviews*, 2(9): 2340-2350.

Paytan, A., Griffith, E.M., 2007. Marine barite: Recorder of variations in ocean export productivity. *Deep-Sea Research Part Ii-Topical Studies in Oceanography*, 54(5-7): 687-705.

Rushdi, A. I., McManus, J., & Collier, R. W., 2000. Marine barite and celestite saturation in seawater. *Marine Chemistry*, 6(9): 19-31

Taylor, S. R., & McLennan, S. M.,1985. *The continental crust : its composition and evolution : an examination of the geochemical record preserved in sedimentary rocks. Stuart Ross Taylor, Scott M. McLennan.* Oxford ; Boston : Blackwell Scientific ; Palo Alto, Calif. : Fistributors, USA and Canada, Blackwell Scientific, 1985.

APPENDIX

TABLE 1: SAMPLE DATA & RESULTS

Depth (cm)	Age (kyr)	Ba (ppm)	bioBa (ppm)	MAR Jacobel	bioBa flux ($\mu g\ cm^{-2}\ kyr^{-1}$)
0	4.9651	545.8983	541.4476731	1.469131455	0.795457808
8	6.51	558.4376	554.2649146	1.458307174	0.808288501
16	8.1293	532.2788	527.8073021	1.595629302	0.842184797
24	10.74977	570.7701	564.7775768	1.525941498	0.861817542
32	12.82096	492.0993	479.8968555	0.960612897	0.460995109
40	16.41955	317.45	310.2478755	1.88841902	0.585877989
48	19.04953	447.6198	439.1210159	1.659209553	0.728593785
56	21.8485	403.4855	394.1929314	1.67222302	0.659178494
64	26.59273	404.7309	396.3540247	1.765464845	0.699749097

Table 1 continued

Depth (cm)	Age (kyr)	Ba (ppm)	bioBa (ppm)	MAR Jacobel	bioBa flux ($\mu g\ cm^{-2}\ kyr^{-1}$)
72	30.07754	396.45	388.413135	1.83779656	0.713824324
80	34.43505	305.3774	297.8506768	2.063176987	0.614518662
88	38.84054	329.2071	322.0476269	2.049993302	0.660195478
96	42.29598	376.3658	368.4648825	1.753202174	0.645993433
104	46.4258	310.528	304.3312496	2.107437449	0.641359072
112	47.99531	311.2037	304.6616755	2.063078986	0.6285411
120	49.25659	329.7279	324.0202783	2.023762901	0.655740218
128	50.48394	343.6308	337.6731853	2.016379422	0.680877262
136	51.70295	353.7469	347.4303331	1.883174509	0.654271947
144	52.95329	391.9591	386.2504583	2.032853735	0.785190687
152	54.32191	415.81	410.2285512	2.089357023	0.857113904

Table 1 continued

Depth (cm)	Age (kyr)	Ba (ppm)	bioBa (ppm)	MAR Jacobel	bioBa flux ($\mu g\ cm^{-2}\ kyr^{-1}$)
160	56.25754	380.878	369.8463264	1.208381594	0.446915494
168	59.97301	359.7726	351.4027907	1.924014725	0.676104144
176	62.5	444.1301	434.9644553	1.75609697	0.763839762
184	65.2	380.5405	370.5367638	1.440945104	0.533923136
192	71.06599	355.3843	348.5515018	1.63866061	0.571157616
200	77.5	434.238	428.1245894	1.566868674	0.670815008
208	81.71422	507.1446	502.0336968	1.725256747	0.866137022
216	84.1	487.2153	480.3879628	1.51201783	0.726355165
224	86.78971	441.7794	436.0680686	1.703446326	0.742818549
232	89.98339	420.6635	413.7933773	1.592578974	0.658998632
240	93.6	394.3997	387.9849499	1.521311249	0.590245869

Table 1 continued

Depth (cm)	Age (kyr)	Ba (ppm)	bioBa (ppm)	MAR Jacobel	bioBa flux ($\mu g\ cm^{-2}\ kyr^{-1}$)
248	96.10677	536.2454	530.9547252	1.574821293	0.836158807
256	98.5	495.8316	491.1755034	1.665052719	0.817833107
272	105.2885	474.2725	469.2263372	1.669600478	0.783420517
288	110	417.814	412.2330092	1.677282657	0.691431277
296	115.6	415.574	410.1362425	1.413259554	0.579628963
316	125.6317	667.0639	662.3547174	1.61288799	1.068303969
372	148.4736	384.2884	375.9114513	1.812954394	0.681510317